Generation, absorption, and transfer of mechanical energy during walking in children

Brian R. Umberger [a,*], Sam Augsburger [b], JoAnne Resig [b], Donna Oeffinger [b], Robert Shapiro [c], Chester Tylkowski [b]

[a] Department of Kinesiology, University of Massachusetts, Amherst, MA, USA
[b] Motion Analysis Laboratory, Shriners Hospital for Children, Lexington, KY, USA
[c] Department of Kinesiology & Health Promotion, University of Kentucky, Lexington, KY, USA

ARTICLE INFO

ABSTRACT

The purpose of this study was to characterize the manner in which net joint moments and non-muscular forces generate, absorb, and transfer mechanical energy during walking in able-bodied children. Standard gait data from seven healthy subjects between 6 and 17 years of age were combined with a dynamic model of the whole body to perform a power analysis based on induced acceleration techniques. These data were used to determine how each moment and force generates energy to, absorbs energy from, and transfers energy among the major body segments. The joint moments were found to induce transfers of mechanical energy between body segments that generally exceeded the magnitudes of energy generation and absorption. The amount of energy transferred by gravitational and velocity-dependent forces was considerably less than for the joint moments. The hip and ankle joint moments had relatively simple power patterns that tended to oppose each other, particularly over the stance phase. The knee joint moment had a more complex power pattern that appeared distinct from the hip and ankle moments. The general patterns of mechanical energy flow were similar to previous reports in adults. The approach described in this paper should provide a useful complement to standard clinical gait analysis procedures.

1. Introduction

In human locomotion, the net moments acting about the joints generate mechanical energy, absorb mechanical energy, and cause mechanical energy to be transferred between body segments [1–4]. A joint moment may generate energy to, or absorb energy from, a body segment that it acts upon directly [3], as well as to distant body segments that it does not act upon [2]. A joint moment may also cause energy to be transferred between body segments, and the magnitude of energy transfer can exceed the magnitude of energy generation/absorption [2]. As with mechanical energy generation and absorption, a joint moment may cause energy to be transferred between body segments that are remote to the joint. For example, an ankle plantar flexor moment may cause energy to be transferred from the thigh to the trunk, even though the ankle moment acts directly on neither the thigh nor the trunk [4]. A better

appreciation of the nature of the energy flows that occur in normal human walking is a critical first step towards better understanding the causes of gait pathology.

Disruption in the flow of mechanical energy through the body is believed to be a major factor contributing to the elevated metabolic cost of walking in children with gait disorders [5–7]. Commonly used methods for investigating mechanical energy flow during gait are based on center of mass kinematics [7], segment kinematics [6], or joint powers [3]. While these techniques may be used to identify abnormal mechanical energy patterns, they provide limited insight as to the *causes* of the abnormal energy patterns. Fregly and Zajac [2] described an alternative power analysis, based on induced acceleration techniques [8], which demonstrates how any force or moment affects the mechanical power of every body segment. Their approach accounted for the flow of energy arising from primarily muscular sources (i.e., net joint moments), as well as non-muscular sources, such as gravitational and velocity-dependent forces (i.e., centrifugal and Coriolis forces). While the original application involved pedaling in adults [2], this technique has also been used to study pedaling in children [9], and has been adapted to study walking in adults [4,10]. The integration of this approach with pediatric gait analysis techniques could lead to a

* Corresponding author at: Department of Kinesiology, 110 Totman Building, 30 Eastman Lane, University of Massachusetts, Amherst, MA 01003-9258, USA. Tel.: +1 413 545 1436; fax: +1 413 545 2906.

E-mail address: umberger@kin.umass.edu (B.R. Umberger).

better understanding of the causes of the elevated cost of walking in gait pathology. However, there have not been, to our knowledge, any reports of induced acceleration-based power analyses of walking in able-bodied children to form a basis for comparison.

Clinical gait analysis is a major component of the overall evaluation and treatment of pediatric gait disorders in conditions such as cerebral palsy [11,12]. The segment-by-segment, free body approach typically used in gait analysis provides the clinician with information on segmental and joint kinematics, as well as joint moments and joint powers. While these standard kinematic and kinetic data are certainly valuable in their own right, they may also be used in conjunction with a dynamic model of the whole body to gain further insights into how the forces and moments that act on the body produce movement. Detailed models of the musculoskeletal system hold tremendous promise in this regard [13]. However, such complex models have seen limited use in clinical practice due to the level of effort involved, the need to account for individual subject characteristics (e.g., bony deformities), and the lack of experience working with musculoskeletal models in most clinical gait laboratories. Whole body models actuated by joint moments represent a more modest level of complexity compared with detailed musculoskeletal models, yet may still provide insights on the mechanics of movement not possible with standard gait analysis techniques [4,10,14–16]. Joint moment-based models eliminate the need to solve the muscle force redundancy problem, and integrate directly with the inverse dynamics approach used in most gait laboratories. In particular, such models may be used to perform induced acceleration-based power analyses [2], providing a better understanding of the energetics of walking than can be inferred from an evaluation of joint powers alone [4,10].

The results of induced acceleration-based power analyses could help in identifying the causes of disorder mechanical energy flows in pediatric gait conditions, and could potentially be integrated directly into standard lab procedures. However, it is first necessary to apply this approach to the analysis of walking in able-bodied children to characterize the patterns of energy flow in this group. Such data would provide important background information for future applications in patient populations. Therefore, the purpose of this investigation was to use experimental kinematic and kinetic data in conjunction with a dynamic model of the whole body to characterize the manner in which net joint moments and nonmuscular forces generate, absorb, and transfer mechanical energy during walking in able-bodied children.

2. Methods

2.1. Subject data

Kinematic and kinetic data were collected from seven able-bodied children (4 females, 3 males) with a mean age of 11.6 ± 3.6 years (range: 6–17 years). Mean body height was 1.52 ± 0.17 m (range: 1.26–1.79 m) and mean body mass was 46.3 ± 13.3 kg (range: 30.0–66.2 kg). The procedures used in this study were in accordance with the Declaration of Helsinki regarding biomedical research involving human subjects, and were approved by the institutional review boards of the University of Massachusetts Amherst and the University of Kentucky.

Experimental data were collected as subjects walked along a 10 m walkway at their self-selected speed (1.17 ± 0.02 m/s). The full-body Cleveland Clinic marker set was used to track the motions of the body segments as the subjects walked across four embedded strain gage force platforms (AMTI Inc., Watertown, MA, USA). Marker trajectories were sampled at 60 Hz using a video-based system (Motion Analysis Corp., Santa Rosa, CA, USA) while ground reaction forces were recorded simultaneously at 960 Hz. The raw
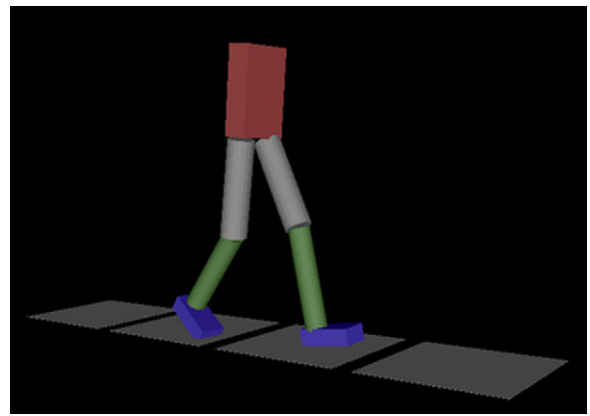

Fig. 1. Diagram of the three dimensional dynamic model used to compute energy flows during gait. The model was scaled to the size of each subject, and the body segments were positioned based on the kinematic data from each subject.

marker and ground reaction force data were processed using the EvaRT software package (Motion Analysis Corp., Santa Rosa, CA, USA), and the marker data were low-pass filtered using a fourth-order, zero phase lag, Butterworth digital filter with a cut-off frequency of 6 Hz. The OrthoTrak software package (Motion Analysis Corp., Santa Rosa, CA, USA) was used to compute three dimensional joint angles, moments, and powers. OrthoTrak was also used to determine the three dimensional positions of joint centers, segment centers of mass, and ground reaction force centers of pressure, for use with the dynamic model. Data from a minimum of three and a maximum of five trails for one complete gait cycle (i.e., heel strike to ipsilateral heel strike) were averaged for each subject before further analysis.

2.2. Dynamic model

A three dimensional dynamic model of the whole body was developed that consisted of seven rigid segments representing the right and left foot, shank, and thigh, as well as a lumped head–arms–trunk (HAT) segment (Fig. 1). The model was actuated bilateral by hip, knee, and ankle joint moments. During model development, we found that the minimum set of actuators necessary for the model to acceptably reproduce experimental data was: hip flexion/extension, hip abduction/adduction, knee flexion/extension, and ankle dorsi/plantar flexion. While these were the only joint axes that were free to rotate, we used the full three dimensional kinematic information from the individual subjects to set the orientation of each segment in the model. For example, knee abduction (valgus) was not an active degree of freedom in the model; however, the orientation of the shank relative to the thigh about the abduction axis was set to match the experimental orientation, and was updated continuously throughout the gait cycle. This approach struck a balance between keeping the model relatively simple, while still taking advantage of the available experimental data.

During periods of ground contact, the foot segments in the model were pinned to the ground at the center of pressure [10,14]. Thus, the feet were free to rotate, but could not translate relative to the ground. The unconstrained model would have possessed 14 degrees of freedom, but due to the foot-ground constraints, the actual number of degrees of freedom varied between 11 during single limb support and 8 during double limb support. The equations of motion for the model were generated using Autolev 4.1 (OnLine Dynamics, Sunnyvale, CA, USA) and coded in Matlab (The MathWorks Inc., Natick, MA, USA). Autolev was also used to derive symbolic expressions for the instantaneous power of each segment

Table 1
Twelve possible ways in which a moment or a force may influence the mechanical energy of the model.

Case	Net	HAT	Limb	Power plot features	Primary energy influences	Generated to/(absorbed from)	Transferred from
1	+	+	+	Net > HAT and Net > Limb	Generation	HAT and Limb	
2	+	+	0	Net = HAT and Limb = 0	Generation	HAT	
3	+	0	+	Net = Limb and HAT = 0	Generation	Limb	
4	+	+	−	HAT > Net and Net > Limb	Generation and Transfer	HAT	Limb to HAT
5	+	−	+	Limb > Net and Net > HAT	Generation and Transfer	Limb	HAT to Limb
6	−	−	−	HAT > Net and Limb > Net	Absorption	(HAT and Limb)	
7	−	−	0	Net = HAT and Limb = 0	Absorption	(HAT)	
8	−	0	−	Net = Limb and HAT = 0	Absorption	(Limb)	
9	−	−	+	Limb > Net and Net > HAT	Absorption and Transfer	(HAT)	HAT to Limb
10	−	+	−	HAT > Net and Net > Limb	Absorption and Transfer	(Limb)	Limb to HAT
11	0	+	−	Net = 0 and HAT = −Limb	Transfer		Limb to HAT
12	0	−	+	Net = 0 and Limb = −HAT	Transfer		HAT to Limb

Net, HAT, and Limb columns refer to the signs of the corresponding power curves in Figs. 5 and 6. A moment or force may generate energy, absorb energy, or transfer energy. Simultaneous energy generation and transfer, or absorption and transfer are also possible. HAT refers to the head, arms, and trunk, and Limb refers to the ipsilateral limb only, as the contralateral limb was excluded from this analysis (see text for details).

in the model [2], which were used in the power analysis described in Section 2.3.

Practical considerations necessitated the use of a simple, one-segment representation of the HAT in the dynamic model. A single HAT segment would likely have been adequate for the current purposes, as arm swing has a relatively minor effect on the mechanics and energetics of walking in able-bodied subjects [17]. However, a single HAT segment could be a limitation in future application involving gait pathology, where there might be abnormal alignment of the trunk or asymmetrical and/or exaggerated motion of the arms. To account for these possibilities, the inertial properties of the single HAT segment in the dynamic model were updated at each time step of the analysis using a second static model. The static model included separate segments representing the trunk, head, upper arms and lower arms (including the hands). The experimental kinematic data for the upper body were used to position the multiple segments in the static model, from which the center of mass location and inertia tensor of the single HAT segment in the dynamic model were determined. Therefore, the single HAT segment in the dynamic model reflected the changing mass distribution of the head, arms, and trunk as the subject walked.

2.3. Power analysis

The three dimensional positions of the predicted joint centers were used to scale the model to the size of each subject, and the center of pressure locations and the body segment angles were used to configure the model at the start of the gait cycle. The experimental moments were then applied to the model one at a time, with all other moments and gravity set to zero, and the mechanical power of each segment was computed. This process was repeated with all moments set to zero and gravity set to 9.81 m/s^2, and again with all moments and gravity set to zero. Together, these latter two conditions allowed for the segment powers due to the gravitational and velocity-dependent forces to be determined. After the segment powers induced by each moment and force had been computed at the current time step, the process was repeated 0.0167 s later in time (corresponding to the 60 Hz sampling frequency), until the end of the gait cycle was reached. The individual moments and gravity were also applied to the model simultaneously to compute the net accelerations of the whole body center of mass. These data were compared with the experimental accelerations computed from the force platform data. For the purposes of data presentation, the powers for the thigh, shank, and foot within a limb were summed, yielding power curves for the HAT, ipsilateral limb, and contralateral limb, due to each net joint moment or non-muscular force. The powers for the HAT and both limbs were further summed to yield the net power.

Following the example of Fregly and Zajac [2], the results of the power analysis were interpreted in terms of the 12 possible ways in which a joint moment may influence the mechanical energy of the HAT and ipsilateral limb (Table 1). A joint moment may potentially generate mechanical energy directly to the HAT, ipsilateral limb, or both, without transferring energy (Table 1, cases 1–3). A joint moment may, at other times, absorb mechanical energy directly from the HAT, ipsilateral limb, or both, without transferring energy (Table 1, cases 6–8). Other possibilities are that a joint moment may transfer mechanical energy between the HAT and ipsilateral limb, while simultaneously generating energy (Table 1, cases 4 and 5) or absorbing energy (Table 1, cases 9 and 10). The remaining possible cases are that a joint moment may transfer mechanical energy between the HAT and ipsilateral limb without generating or absorbing energy (Table 1, cases 11 and 12). For simplicity, the contralateral limb was excluded from the formal energy flow analysis. Including the contralateral limb would have greatly complicated the logic of Table 1 by adding many more possible combinations, when in fact, the power of the contralateral limb was usually quite low. For the few instances in which the contralateral limb power was not low, the interpretations were handled on an ad hoc basis.

3. Results

3.1. Subject data

The traditional gait variables, consisting of hip, knee, and ankle joint angles, moments, and powers, are shown for the subjects in Fig. 2. The between-subject variability, reflected by the magnitudes of the standard deviation envelopes, was greater for the hip variables than the ankle or knee, yet was still relatively small, despite the wide ranges in age and body size among the subjects. All moment and power variables (joint, net, and segment powers) were expressed relative to body mass. However, an alternative approach is to express gait data in dimensionless form [18]. We repeated all of our analyses with our variables computed in dimensionless form and confirmed that the manner of data presentation did not change any of the general patterns in the data, nor the conclusions drawn from them.

3.2. Model evaluation

The performance of the model was evaluated by comparing the accelerations of the whole-body center of mass with the corresponding values in the subjects (Fig. 3), and by comparing the net powers computed using the model with the joint powers in the subjects (Fig. 4). The center of mass accelerations computed with the model were within one standard deviation of the mean values
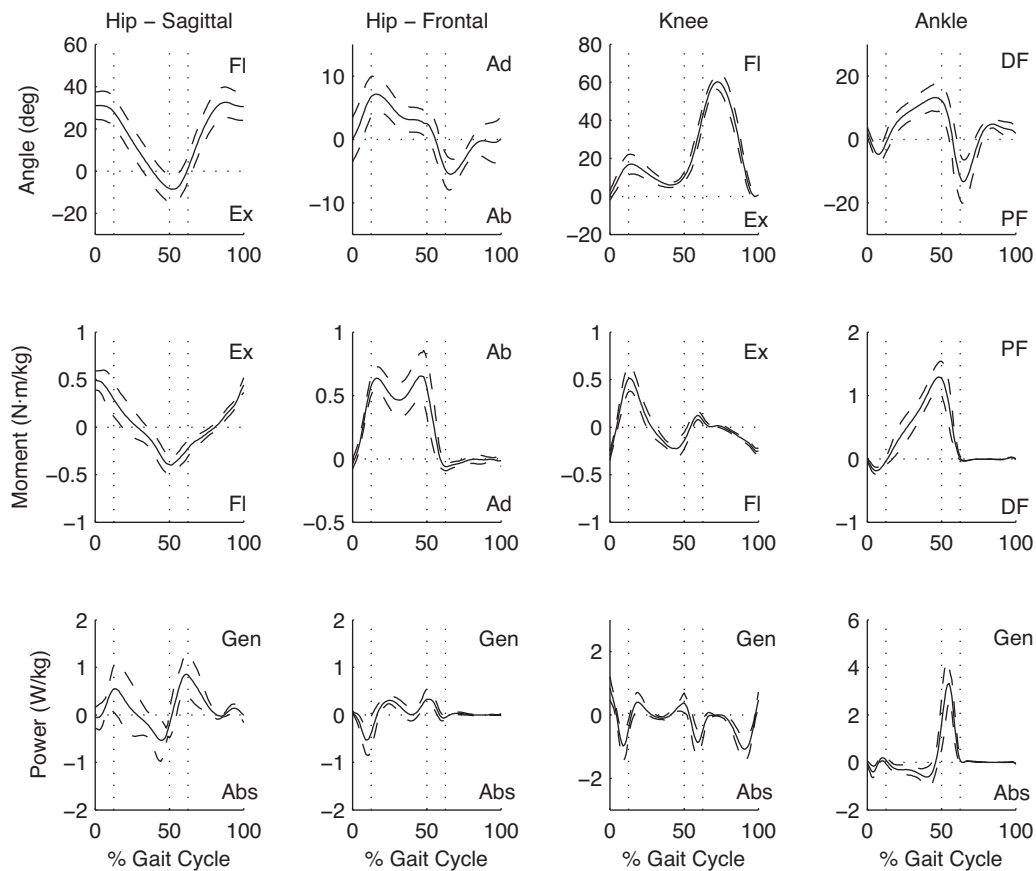
Fig. 2. Joint angles, moments, and powers for the experimental subjects. Data are means ± 1 S.D. The dotted vertical lines from left to right indicate: contralateral limb toe off, contralateral limb heel strike, and ipsilateral limb toe off. Zero and 100% of the gait cycle correspond to ipsilateral limb heel strike. Fl, flexion; Ex, extension; Ad, adduction; Ab, abduction; DF, dorsiflexion; PF, plantar flexion; Gen, generation; Abs, absorption.

in the subjects for all but a brief period around the end of double-limb support (Fig. 3; around 10 and 60% of the gait cycle). The net powers in the model were within one standard deviation of the mean subject joint powers over the entire gait cycle (Fig. 4).

3.3. Power analysis

The mechanical power distributions due to the moments and forces acting on the model are shown in Fig. 5. The ipsilateral hip, knee, and ankle joint moments had substantial energetic effects on the HAT, ipsilateral limb, and in some cases, the contralateral limb (e.g., hip around 50% of the gait cycle in Fig. 5A). The segment powers induced by the joint moments, and the energy transfers between segments (occurring when signs of the segment powers were opposite), were considerably greater in magnitude than the net powers, with only a few exception (e.g., ankle around 55% of the gait cycle in Fig. 5C). Thus, in addition to adding or removing energy from the body as a whole, the joint moments played a major role in redistributing mechanical energy among the body segments. The velocity-dependent forces and gravitational forces could not perform net work on the body, but did serve to transfer small amounts of energy between body segments over the gait cycle (Fig. 5D and E).

In Fig. 6, the joint angle and moment data from Fig. 2 are combined with the joint moment power distributions from Fig. 5. The numbers marking specific regions of the curves in the bottom three panels (Fig. 6G–I) correspond to the possible cases of mechanical energy generation, absorption, and transfer identified in Table 1. Periods of the gait cycle with relatively low powers are not marked. At the beginning of the gait cycle, the hip joint moment generated

energy to the HAT (Fig. 6G), and transferred energy from the ipsilateral limb to the HAT (case 4). This was followed by an interval with relatively low powers (unmarked). During the latter half of the stance phase, the hip joint moment first absorbed energy from the HAT and contralateral limb, while transferring energy to the ipsilateral limb (case 9), and then switched to generating energy directly to the ipsilateral limb, while maintaining the same energy transfer profile (case 5). This pattern of energy flow (case 5) continued into the early part of the swing phase. During the mid-to-late swing phase, the hip joint moment transferred energy from the ipsilateral limb to the HAT (and to a lesser extent the contralateral limb), with almost no net generation or absorption (case 11). The hip joint moment was the only force or moment that had a meaningful influence on the power of the contralateral limb, primarily around the middle of gait cycle.

The knee joint moment had the most complex pattern of energy flow (Fig. 6H), yet it was dominated by only two of the possible cases (5 and 10). For the period right around ipsilateral limb heel strike, the knee joint moment generated energy to the ipsilateral limb, and transferred energy from the HAT to the ipsilateral limb (case 5). This was followed by a brief interval where the knee joint moment absorbed energy from the ipsilateral limb, while transferring energy from the ipsilateral limb to the HAT (case 10). Over the next brief interval, the knee joint moment generated energy to the HAT, while transferring energy from the ipsilateral limb to the HAT (case 4). This was followed by a longer period where the knee joint moment generated a relatively small amount of energy to the ipsilateral limb, and transferred energy from the HAT (and to a lesser extent from the contralateral limb) to the ipsilateral limb (case 5). At the end of the stance phase, there was another brief interval
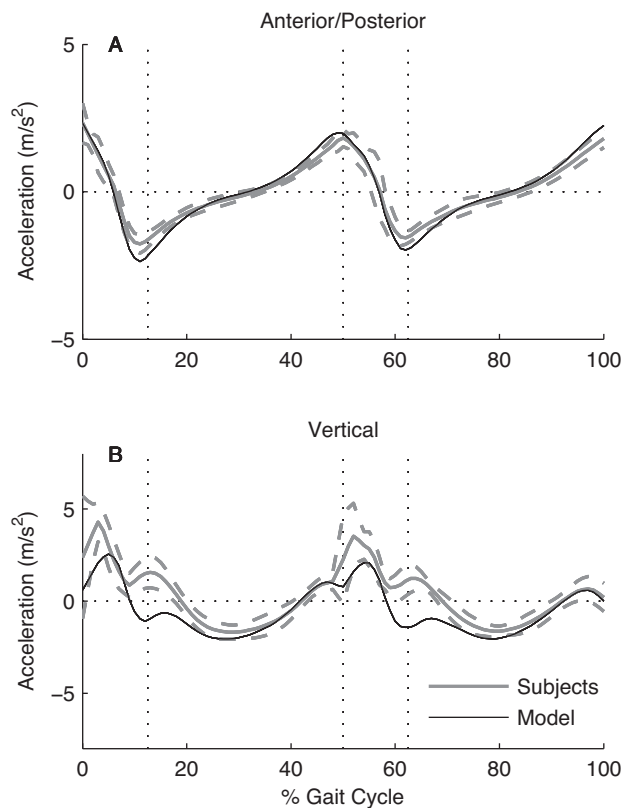
Fig. 3. Vertical (A) and anterior–posterior (B) accelerations of the whole body center of mass for the experimental subjects, and the corresponding accelerations derived from the model. The dotted vertical lines from left to right indicate: contralateral limb toe off, contralateral limb heel strike, and ipsilateral limb toe off. Zero and 100% of the gait cycle correspond to ipsilateral limb heel strike. Data for subjects are means ± 1 S.D.; data for model are means across subjects.

where the knee joint moment absorbed energy from the ipsilateral limb, while transferring energy from the ipsilateral limb to the HAT (case 10). The knee joint moment powers were low during much of the swing phase, but returned, just before heel strike, to the pattern where energy was generated directly to the ipsilateral limb, and transferred from the HAT to the ipsilateral limb (case 5).

At the beginning of the stance phase, the ankle joint moment absorbed energy from the HAT (Fig. 6I), while transferring energy from the HAT to the ipsilateral limb (case 9). This was followed by a period with relatively little energy flow (unmarked). Around the middle of the stance phase, the ankle joint moment absorbed energy from the ipsilateral limb, while transferring energy from the ipsilateral limb to the HAT (case 10). This was followed by a brief interval where the ankle joint moment continued to transfer energy from the ipsilateral limb to the HAT, but also generated energy directly to the HAT (case 4). The end of the stance phase was characterized by an even shorter period where the ankle joint moment generated energy directly to both the HAT and the ipsilateral limb (case 1). Energy flows due to the ankle joint moment during the swing phase were small in magnitude.

4. Discussion

In this study, we combined gait kinematic and kinetic data with a dynamic model of the whole body to determine how net joint moments, gravitational forces, and velocity-dependent forces influence the mechanical energetics of the body during walking in able-bodied children. The joint moments were found to induce large transfers of mechanical energy, primarily between the ipsilateral limb and the HAT. With few exceptions, the magnitudes
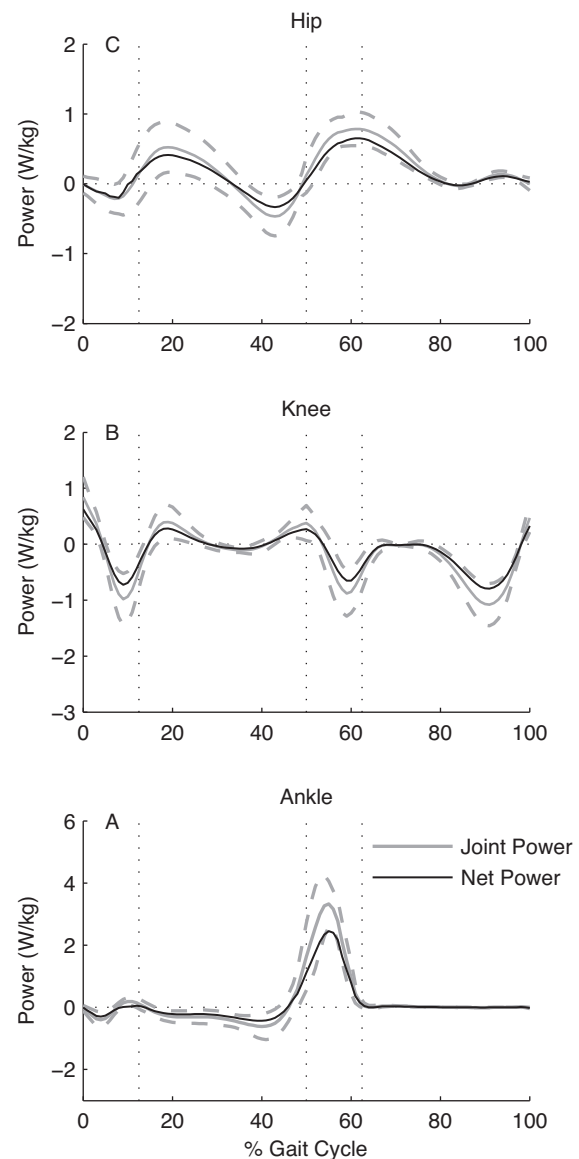

Fig. 4. Hip (A), knee (B), and ankle (C) joint powers for the experimental subjects, and corresponding net powers derived from the model. The dotted vertical lines from left to right indicate: contralateral limb toe off, contralateral limb heel strike, and ipsilateral limb toe off. Zero and 100% of the gait cycle correspond to ipsilateral limb heel strike. Net power is equal to sum of the powers for HAT and both limbs. Data for hip are the sum of sagittal and frontal plane powers. Data for subjects are means ± 1 S.D.; data for model are means across subjects.

of these energy transfers exceeded the magnitudes of mechanical energy generation and absorption by the joint moments. The gravitational and velocity-dependent forces also induced energy transfers, but the magnitudes of these energy flows were smaller than for the joint moments. These results build upon earlier work focused on walking in adults [4,10] and on other locomotor tasks in children and adults [2,9].

We found the same general trends in the distributions of segment powers in our subjects as Siegel et al. [4] reported in adults. This finding is consistent with the notion that able-bodied children over the age of 5 years have an essentially mature gait pattern [19], subject only to differences in the magnitudes of certain gait variables (e.g., peak ankle moment, negative joint work) associated with children at the lower end of our age range [20,21]. The powers with the greatest magnitudes for both energy generation and transfer were associated with the ankle joint moment (Fig. 5C). The
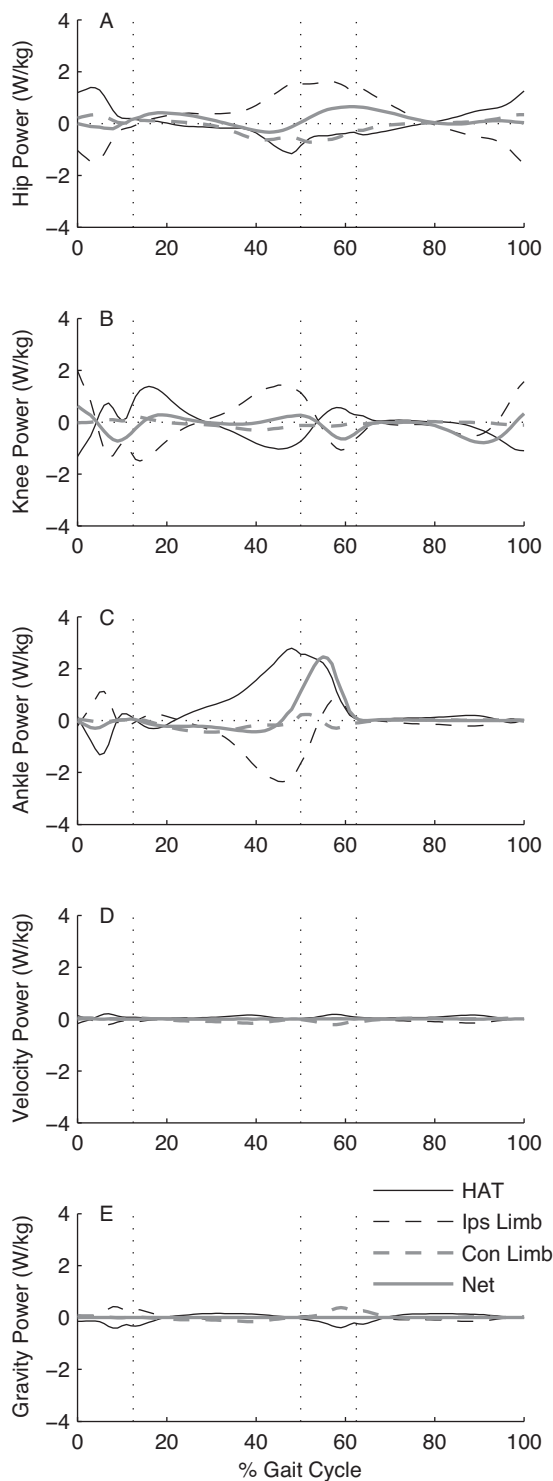
Fig. 5. Mechanical power distributions due to the hip joint moment (A), knee joint moment (B), ankle joint moment (C), velocity-dependent forces (D), and gravitational forces (E). The dotted vertical lines from left to right indicate: contralateral limb toe off, contralateral limb heel strike, and ipsilateral limb toe off. Zero and 100% of the gait cycle correspond to ipsilateral limb heel strike. Data are means across subjects.

large ankle joint power burst near the end of the stance phase (solid gray line in Fig. 5C), often associated with the action of "pushing off" against the ground, is one of the most characteristic features of able-bodied gait. Our analysis revealed that the ankle joint moment generates energy directly to the massive HAT during this interval

(Fig. 6I). However, similar to the case in adults [4], we found that the ankle moment also transfers a considerable amount of energy to the HAT over an interval spanning nearly 25% of the gait cycle immediately before push off, even though ankle joint power is negative (Fig. 6I). Thus, the ankle plantar flexor muscles play a critical role in maintaining the energy of the HAT well before the net ankle power becomes positive. This more detailed understanding of ankle muscle function may have important implications for planning and interpreting the outcomes of surgical procedures designed to treat conditions such as equine contractures [12].

While powers associated with the ankle joint moment had the greatest absolute magnitudes, the hip joint moment had the greatest effect on the energetics of the contralateral limb (Fig. 5A). From approximately 30–70% of the gait cycle, the hip joint moment transferred similar amounts of energy to the ipsilateral limb from the contralateral limb *and* from the HAT (Fig. 6G). The knee and ankle joint moments had smaller effects on the contralateral limb than the hip moment, in both absolute and relative terms (Fig. 5B and C). The hip joint moment also dominated the energetics of the ipsilateral limb during the swing phase. The hip moment transferred energy from the HAT to the limb, while simultaneously generating energy directly to the limb in the first half of the swing phase (Fig. 6G). During the second half of the swing phase, the hip joint moment primarily transferred energy from the limb to the HAT. This change in role corresponded with the change in sign of the hip joint moment from flexor to extensor around the middle of the swing phase (Fig. 6D). Only the knee joint moment made a contribution of similar magnitude to that of the hip joint moment during the swing phase. However, this action by the knee moment was limited to the final quarter of the swing phase, and had the opposite energetic effect as the hip moment, transferring energy from the HAT to the limb (Fig. 6H).

Over the stance phase, the powers due to the hip (Fig. 5A) and ankle (Fig. 5C) joint moments had relatively simple patterns, which were nearly opposite in sign, if not equal in magnitude. The powers due to the knee joint moment (Fig. 5B), on the other hand, exhibited a more complex pattern that did not follow uniformly with the powers for either the hip or ankle moments. An important feature of the power curves associated with the knee joint moment occurred around 15% of the gait cycle, where the knee moment appeared to play a key role in maintaining the mechanical energy of the HAT. At this point in the gait cycle, the knee moment acted to transfer energy from the ipsilateral limb to the HAT, while the hip and ankle moments had little effect on the energetics of the body segments. This action by the knee joint moment corresponded approximately with the first knee extension moment peak (Fig. 6E). A related observation, which is consistent with results in adults [4], is that the powers for the HAT due to each joint moment approximately follow the patterns of the corresponding joint moments (Fig. 6). Thus, extensor moments primarily caused energy to flow into the HAT, while flexor moments primarily caused energy to flow out of the HAT. Moreover, the powers of the HAT segment follow more closely with the patterns of the joint moments than with the patterns of the corresponding joint powers. While the correspondence of HAT powers with the joint moments may provide a useful rubric, it is important to note that the joint moments provide no information on whether the increases and decreases in HAT energy reflect direct energy generation/absorption, transfer, or both. The way in which a joint moment, or any other force, influences the mechanical powers of the HAT and limb is through the contribution that it makes to the intersegment hip joint reaction force, which is contained implicitly in our model formulation. As noted previously [2], it is necessary to utilize the equations of motion for the entire system (whole body in our case) in order to fully decompose how each moment or force causes energy to flow into and out of each body segment. This level of insight is not possible based solely on
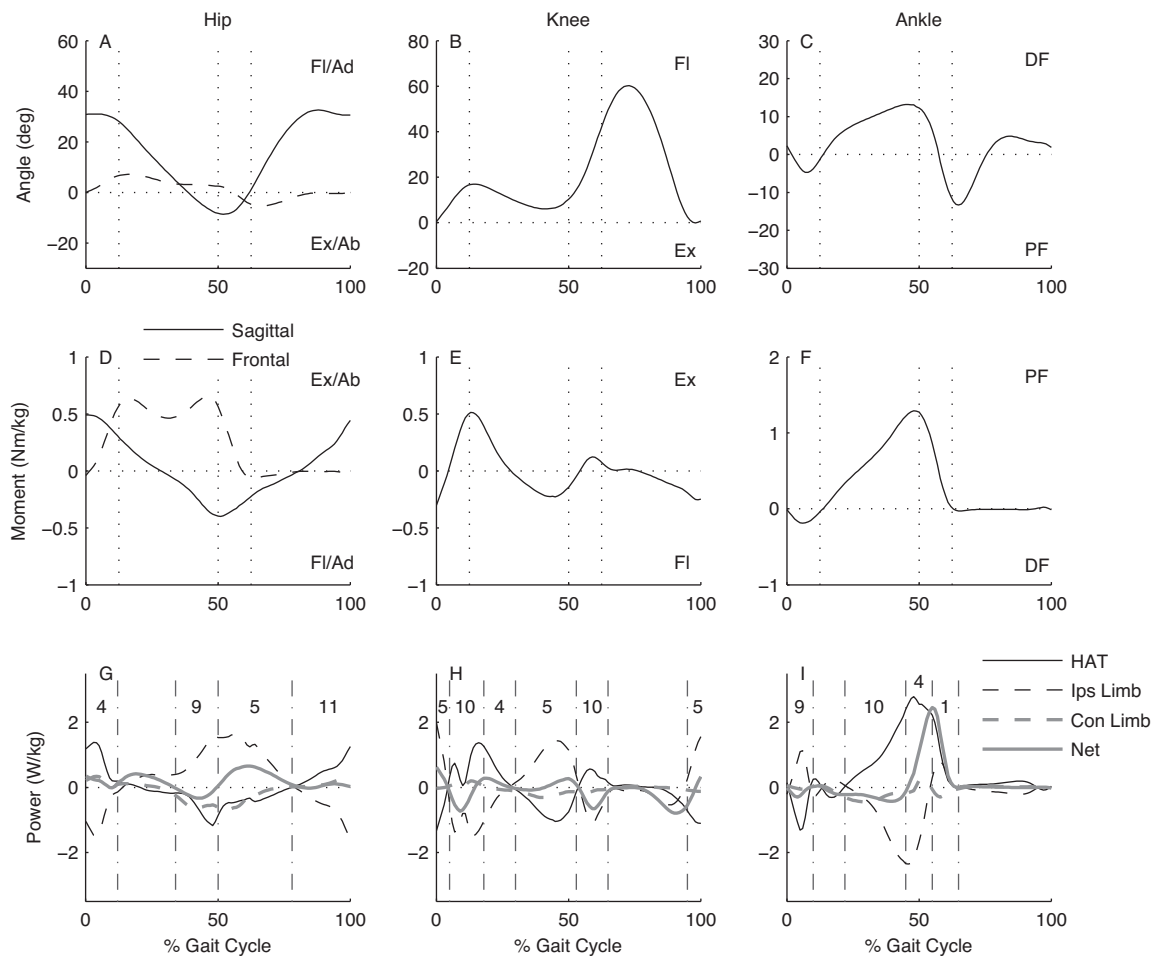
Fig. 6. Joint angles (A–C) and moments (D–F) for the hip, knee, and ankle, and the mechanical power distributions due to the moments for these joints (G–I). The dotted vertical lines in panels A–F from left to right indicate: contralateral limb toe off, contralateral limb heel strike, and ipsilateral limb toe off. Zero and 100% of the gait cycle correspond to ipsilateral limb heel strike. The numbers in panels G–I correspond to specific patterns of mechanical energy flow identified in Table 1. The dash–dot vertical lines in panels G–I indicate transitions between specific cases of energy flow.

moments and powers from a free-body inverse dynamics analysis [1,3].

Combining the current analyses with metabolic data may prove useful in understanding why the cost of walking is higher in smaller children, and why it is further elevated in many gait disorders. The cost of walking would be expected to correlate positively with mechanical energy generation, and correlate negatively with mechanical energy transfer. However, efforts to explain differences in the cost of walking in children using traditional work and energy transfer measures have thus far met with limited success [22]. Joint moments serve to transfer mechanical energy between segments during walking, to an extent that generally exceeds the generation and absorption of energy. The energy transfer role played by each joint moment is likely critical in maintaining the energetic state of the body to effect smooth, coordinated locomotion. Any disruption in the normal transfer of energy among body segments may need to be compensated for by additional mechanical energy generation by the muscles, which will exact a metabolic cost. The ability of the present approach to identify how each joint moment influences the instantaneous mechanical power of all body segments should be helpful both in understanding why the cost of walking changes with growth and development, and in identifying the causes of elevated cost in gait pathologies.

Given the similarities between our study and that of Siegel et al. [4], it is worth noting some differences in how the data are presented in the two studies. We chose to present our results in terms of the segment powers for the HAT, ipsilateral limb, contralateral limb, and the net power (Figs. 5 and 6), as we felt this approach provided a holistic view of how each force and moment contributes to energy flow throughout the body. This approach also facilitated the systematic analysis of mechanical energy flow (Table 1 and Fig. 6G–I). In contrast, Siegel et al. [4] reported powers for the HAT and ipsilateral thigh, shank, and foot (their Fig. 2), but not for the ipsilateral limb as a whole, and not for the contralateral limb or the net power (net power was reported, but in a separate graph). Despite these differences, it is relatively easy to compare some of the major results between the two studies. Our ipsilateral limb data represent the sum of the powers for the ipsilateral thigh, shank, and foot. The primary justification for grouping these segments was that Siegel et al. [4] found the thigh and shank powers tended to vary together, while the foot powers tended to be small in magnitude. We found the same to be true in our data. It is straightforward to separate out the thigh, shank, and foot segment powers, but only at the expense of complicating the resulting graphs, especially if data for the contralateral limb and the net power are also included. We feel that evaluating the net power simultaneously with the powers for both limbs and the HAT is key to understanding the energetic role of each joint moment. However, this does not preclude the possibility that in certain cases, such as in pathological gait, it may be informative to analyze the individual segments within a limb.

The quality of the model results obtained in this study were evaluated by comparing the accelerations of the whole body

center of mass predicted by the model with the same accelerations measured in the subjects (Fig. 3), and by comparing the net powers determined with the model to the joint powers computed for the subjects (Fig. 4). The center of mass accelerations in the subjects were obtained directly from force platform data, and the joint powers in the subjects were determined as part of the inverse dynamics analysis (i.e., joint moment × joint angular velocity). The center of mass accelerations in the model fell within one standard deviation of the experimental mean, except for a span of about 10% of the gait cycle around each of the toe-off events. The discrepancy was greater for the vertical component than the anterior–posterior component (Fig. 3). It is important to note, though, that despite the center of mass accelerations being more than one standard deviation beyond the mean for part of the gait cycle, the net powers remained within one standard deviation of the mean joint powers across the entire gait cycle (Fig. 4). This was possible because the model powers were evaluated separately at each time step based on the experimental gait data. Thus, any errors in the accelerations were not allowed to propagate forward and grow over time. The discrepancies in the center of mass accelerations were likely due to simplifications that were made in the model, both in terms of the model structure and the foot-ground interface. Despite some discrepancies, the model center of mass accelerations and net powers agreed with the corresponding experimental data to an extent that we felt justified the level of complexity of the model. Part of our motivation was to develop a model that could be used routinely in a clinical gait setting. Thus, there was a need to balance model complexity and simplicity. Better agreement with the measured data could presumably be obtained by using a more complex foot-ground interface, including more degrees of freedom and actuators, employing more sophisticated model calibration procedures [16], or by using optimal estimation techniques [23]. However, we do not feel that the added complexity would be justified for our present purposes.

The primary limitation of the present approach, which is shared by all joint moment-based models [4,10,14–16], is that no information is provided on the roles played by individual muscles. For example, it would not be possible to identify differential roles of the soleus and gastrocnemius without using a model including individual muscle actuators [24]. Moreover, all of the same cautions that apply to the interpretation of data from a traditional inverse dynamics analysis [25] apply to results obtained with the current model. We view the approach described here as a direct extension of standard gait analysis procedures, which currently play a key role in the evaluation and treatment of children with cerebral palsy and other gait disorders. The present analyses, based on induced acceleration techniques [2,4], go beyond joint moments and powers, and should provide the clinician with additional useful information on the energetics of locomotion. The approach described herein would not be a replacement for using a more detailed, subject-specific musculoskeletal model to evaluate the gait of a particular patient [13]. Such complex analyses may become routine in the future, but have not yet found their way into routine clinical practice. Instead, the present approach represents an opportunity to gain additional insight into the mechanics and energetics of walking, in a way that integrates with current gait analysis procedures, and does not require any additional data collection or place any additional burden on the patient.

This study extends our knowledge of the energetics of locomotion by applying an induced acceleration-based power analysis to the study of walking in able-bodied children. The general similarity of our results to those reported previously in adults suggests that the present data are representative. However, it will be necessary to study a larger number of subjects to establish normative data. While our sample covers a wide age range, it will also be helpful to have data on children younger than 6 years old, to evaluate whether there are important changes in mechanical energy transfer during early development. Finally, for the procedures to be truly useful in a clinical setting, we will need to evaluate the feasibility of performing the analyses in children with gait pathology.

Conflict of interest statement

None of the authors had any conflicts of interest related to this study.

References

[1] Caldwell GE, Forrester LW. Estimates of mechanical work and energy transfers: demonstration of a rigid body power model of the recovery leg in gait. Med Sci Sports Exerc 1992;24:1396–412.

[2] Fregly BJ, Zajac FE. A state–space analysis of mechanical energy generation, absorption, and transfer during pedaling. J Biomech 1996;29:81–90.

[3] Robertson DG, Winter DA. Mechanical energy generation, absorption and transfer amongst segments during walking. J Biomech 1980;13:845–54.

[4] Siegel KL, Kepple TM, Stanhope SJ. Joint moment control of mechanical energy flow during normal gait. Gait Posture 2004;19:69–75.

[5] Campbell J, Ball J. Energetics of walking in cerebral palsy. Orthop Clin North Am 1978;9:374–7.

[6] Olney SJ, Costigan PA, Hedden DM. Mechanical energy patterns in gait of cerebral palsied children with hemiplegia. Phys Ther 1987;67:1348–54.

[7] Bennett BC, Abel MF, Wolovick A, Franklin T, Allaire PE, Kerrigan DC. Center of mass movement and energy transfer during walking in children with cerebral palsy. Arch Phys Med Rehabil 2005;86:2189–94.

[8] Zajac FE, Gordon ME. Determining muscle's force and action in multi-articular movement. Exerc Sport Sci Rev 1989;17:187–230.

[9] Korff T, Jensen JL. Age-related differences in adaptation during childhood: the influences of muscular power production and segmental energy flow caused by muscles. Exp Brain Res 2007;177:291–303.

[10] Riley PO, Della Croce U, Kerrigan DC. Propulsive adaptation to changing gait speed. J Biomech 2001;34:197–202.

[11] Gage JR, Koop SE. Clinical gait analysis: application to management of cerebral palsy. In: Allard P, Stokes I, Blanchi J, editors. Three dimensional analysis of human movement. Champaign, IL: Human Kinetics; 1995. p. 349–62.

[12] Tylkowski CM, Horan M, Oeffinger DJ. Outcomes of gastrocnemius–soleus complex lengthening for isolated equinus contracture in children with cerebral palsy. J Pediatr Orthop 2009;29:771–8.

[13] Arnold AS, Delp SL. Computer modeling of gait abnormalities in cerebral palsy: application to treatment planning. Theor Issues Ergon Sci 2005;6: 305–12.

[14] Kepple TM, Siegel KL, Stanhope SJ. Relative contributions of the lower extremity joint moments to forward progression and support during gait. Gait Posture 1997;6:1–8.

[15] Nott CR, Zajac FE, Neptune RR, Kautz SA. All joint moments significantly contribute to trunk angular acceleration. J Biomech 2010;43:2648–52.

[16] Reinbolt JA, Haftka RT, Chmielewski TL, Fregly BJ. A computational framework to predict post-treatment outcome for gait-related disorders. Med Eng Phys 2008;30:434–43.

[17] Umberger BR. Effects of suppressing arm swing on kinematics, kinetics, and energetics of human walking. J Biomech 2008;41:2575–80.

[18] Hof AL. Scaling gait data to body size. Gait Posture 1996;4:222–3.

[19] Sutherland D. The development of mature gait. Gait Posture 1997;6:163–70.

[20] Cupp T, Oeffinger D, Tylkowski C, Augsburger S. Age-related kinetic changes in normal pediatrics. J Pediatr Orthop 1999;19:475–8.

[21] Van de Walle P, Desloovere K, Truijen S, Gosselink R, Aerts P, Hallemans A. Age-related changes in mechanical and metabolic energy during typical gait. Gait Posture 2010;31:495–501.

[22] Frost G, Dowling J, Bar-Or O, Dyson K. Ability of mechanical power estimations to explain differences in metabolic cost of walking and running among children. Gait Posture 1997;5:120–7.

[23] Remy CD, Thelen DG. Optimal estimation of dynamically consistent kinematics and kinetics for forward dynamic simulation of gait. J Biomech Eng 2009;131:031005.

[24] Neptune RR, Kautz SA, Zajac FE. Contributions of the individual ankle plantar flexors to support, forward progression and swing initiation during walking. J Biomech 2001;34:1387–98.

[25] Winter DA. Biomechanics and motor control of human movement. New York: John Wiley & Sons; 1990.